Scattering through fruits during ripening: laser speckle technique correlated to biochemical and fluorescence measurements

Rana Nassif, Fabrice Pellen, Christian Magné, Bernard Le Jeune, Guy Le Brun, Marie Abboud

Scattering through fruits during ripening: laser speckle technique correlated to biochemical and fluorescence measurements

Rana Nassif,[1,2,*] **Fabrice Pellen,**[1] **Christian Magné,**[3] **Bernard Le Jeune,**[1] **Guy Le Brun,**[1,4] **and Marie Abboud**[2,5]

[1]*Université de Brest, UEB, EA 938 Laboratoire de Spectrométrie et Optique Laser, 6 avenue Le Gorgeu, C.S. 93837, 29238, Brest Cedex 3, France*
[2]*Physics department, Faculty of science, Saint Joseph University, B.P. 11-514 - Riad El Solh Beirut 1107 2050, Lebanon*
[3]*Université de Brest, UEB, EA 2219 Geoarchi, Brest, France*
[4]*guy.LeBrun@univ-brest.fr*
[5]*marie.abboud@fs.usj.edu.lb*

[*]*rana.nassif@univ-brest.fr*

Abstract: This paper reports monitoring fruits maturation using speckle technique. Performed measurements aim the assessing of biological inner fruit variation effect on the speckle image. We show that the speckle grain size is both affected by the glucose level inside the fruits and by the chlorophyll content. Moreover, the determination of circular polarization degree and circular grain size indicate that a Rayleigh diffusion regime gradually becomes predominant in fruits. Principal component analysis is used to highlight high correlation between results and strengthen the establishment of speckle as a novel non invasive method to monitor fruits ripening.

OCIS codes: (030.6140) Speckle; (290.5850) Scattering; (290.1990) Diffusion; (260.5430) Polarization.

References and links

1. F. R. Harker, J. H. Maindonald, and P. J. Jackson, "Penetrometer Measurement of Apple and Kiwifruit Firmness: Operator and Instrument Differences," J. Am. Soc. Horticult. Sci. **121,** 927–936 (1996).
2. A. d. J. Maurizio Ventura, H. de Putter, and F. P. Roelofs, "Non-destructive determination of soluble solids in apple fruit by near infrared spectroscopy," Postharvest Biol. Technol. **14**, 21–27 (1998).
3. A. Zdunek, L. Muravsky, L. Frankevych, and K. Konstankiewicz, "New nondestructive method based on spatial-temporal speckle correlation technique for evaluation of apples quality during shelf-life," Int. Agrophys. **21**, 305–310 (2007).
4. G. F. Rabelo, R. A. Braga Junior, I. M. Fabbro, M. R. Trivi, H. J. Rabal, and R. Arizaga, "Laser speckle techniques in quality evaluation of orange fruits," Revista Brasileira de Engenharia Agricola e Ambiental **9**, 570–575 (2005).
5. M. Pajuelo, G. Baldwin, H. Rabal, N. Cap, R. Arizaga, and M. Trivi, "Bio-speckle assessment of bruising in fruits," Opt. Lasers Eng. **40**, 13–24 (2003).
6. B. Cordenunsi and F. Lajolo, "Starch Breakdown during Banana Ripening: Sucrose Synthase and Sucrose Phosphate Synthase," J. Agric. Food Chem. **43**, 347–351 (1995).
7. J. W. Goodman, "Statistical Properties of Laser Speckle Patterns," in *Laser speckle and related phenomena*, **9** in series Topics in Applied Physics, J. C. Dainty, Ed., (Springer-Verlag, 1984).

#171813 - $15.00 USD Received 13 Jul 2012; revised 30 Aug 2012; accepted 31 Aug 2012; published 3 Oct 2012

8. Q. B. Li and F. P. Chiang, "Three-dimensional dimension of laser speckle," Appl. Opt. **31**, 6287–6291 (1992).
9. S. Morgan and M. Ridgway, "Polarization properties of light backscattered from a two layer scattering medium," Opt. Express **7**, 395–402 (2000).
10. Y. Piederrière, F. Boulvert, J. Cariou, B. Le Jeune, Y. Guern, and G. Le Brun, "Backscattered speckle size as a function of polarization: influence of particle-size and concentration," Opt. Express **13**, 5030–5039 (2005).
11. S. G. Demos and R. R. Alfano, "Optical polarization imaging," Appl. Opt. **36**, 150–155 (1997).
12. C. Liu, Y. Song, D. Zhang, and H. Zhang, "On-spot evaluation of maturity stage of fruits based on 655 nm laser-induced photoluminescence of chlorophyll-α," Metamaterials **9**, 57–59(2006).
13. E. W. Yemm and A. J. Willis, "The estimation of carbohydrates in plant extracts by anthrone," Biochem. J. **57**, 508–514 (1954).
14. C. Magné, M. Bonenfant-Magné, and J.-C. Audran, "Nitrogenous indicators of postharvest ripening and senescence in apple fruit (malus domestica borkh. cv. granny smith)," Int. J. Plant Sci. **158**, 811–817 (1997).
15. H. K. Lichtenthaler and C. Buschmann, "Chlorophylls and Carotenoids: Measurement and Characterization by UV-VIS Spectroscopy," in *Current Protocols in Food Analytical Chemistry*, (John Wiley & Sons, Inc., 2001) 705–758.
16. H. C. van de Hulst, "Rayleigh-Gans scattering," in *Light Scattering by Small Particles*, (Dover Publications, Inc., 1981) 85–88.
17. J. S. Maier, S. A. Walker, S. Fantini, M. A. Franceschini, and E. Gratton, "Possible correlation between blood glucose concentration and the reduced scattering coefficient of tissues in the near infrared," Opt. Lett. **24**, 2062–2064 (1994).
18. Y. Piederrière, J. Cariou, Y. Guern, B. Le Jeune, G. Le Brun, and J. Lortrian, "Scattering through fluids: speckle size measurement and monte carlo simulations close to and into the multiple scattering," Opt. Express **12**, 176–188 (2004).
19. H. Abdi and L. J. Williams, "Principal component analysis," WIREs Comp. Stat. **2**, 433–459 (2010).

1. Introduction

The use of non invasive and non destructive methods to follow the ripening of fruits and vegetables is a subject of interest in agriculture. The main purpose is to characterize the best day to harvest the fruits, to follow the ripening of climacteric fruits when they ripen off-tree and eventually to predict the optimum storage life. Several methods are currently developed and used. Some are destructive, like the measurement of the sugar content or the use of the penetrometer [1] and some are not, such as acoustic method and infrared spectrometry [2].
Biospeckle is a novel non invasive method recently applied to this field. Speckle is a phenomenon produced by laser illumination of a medium, resulting from the temporally non stationary interference of light scattered by diffusing objects. This method proved its ability to monitor fruits ripening and to assess bruising in fruits using correlation between images [3], Time History of a Speckle Pattern method (THSP) [4] or the Weighted Generalized Differences method (WGD) [5].
In this paper, we report results based on speckle polarization analysis correlated to fruits content variation obtained from biochemical and fluorescence measurements. In our work, and unlike previous studies, we consider fruits as scattering media presenting variable sizes of scatterers along maturation. Thus, our issue is to characterize these diffusers, their relative size and their variation on the speckle image. This approach, which is to the best of our knowledge adopted for the first time, allows us to link speckle image variation and diffusion properties evolution to fruit inner physiology. In section 2, we present the speckle grain size estimation and the polarization analysis used to characterize the fruit composition during different maturation stages. The speckle experimental setup, fluorescence and biochemical measurements are described in section 3. Section 4 is dedicated to results which are discussed and inter-correlated using the principal component analysis method. Our conclusions are drawn in section 5.

2. Theory

Fruits are a complex environment presenting different size distributions of molecules depending on the maturation level. Green fruits are rich in starch chains $(C_6H_{12}O_5)_n$ which are rela-

#171813 - $15.00 USD Received 13 Jul 2012; revised 30 Aug 2012; accepted 31 Aug 2012; published 3 Oct 2012

tively large (0.1 to 200 microns), as well as pectin, organic acids and amino acids. During fruit maturation process, starch and amino acids are hydrolyzed to carbohydrates such as glucose $C_6H_{12}O_6$ [6]. Unlike starch, these are small molecules, on the order of few nm. Any modification of the fruit inner constituents affects its optical properties, specially the absorption and the scattering coefficients. Thus, one can monitor different fruit maturation stages using speckle images and parameters, namely the speckle grain size and the light polarization degree.
The speckle grain size is estimated using the normalized auto-covariance function of the speckle intensity pattern I(x,y) obtained in the observation plane (x,y) of the camera. This function c_I(x,y) corresponds to the normalized autocorrelation function of the intensity. It has a zero base and its width provides a reasonable measurement of the average width of a speckle grain [7]. It is calculated based on the Wiener-Khintchine theorem. From the intensity distribution of the measured speckle, normalized c_I(x,y) is described in Eq.1:

$$c_I(x,y) = \frac{FT^{-1}[|FT[I(x,y)]|^2] - \langle I(x,y)\rangle^2}{\langle I^2(x,y)\rangle - \langle I(x,y)\rangle^2} \tag{1}$$

where FT is the Fourier Transform and $\langle\rangle$ is a spatial average. The horizontal dimension of the speckle grain denoted dx is the full width at half maximum (FWHM) of the horizontal profile of c_I(x,y) and the vertical one dy is the FWHM of the vertical profile of c_I(x,y).
Speckle grain size depends on the wavelength λ, the distance of observation between the camera and the illuminated sample D and the diameter of the circularly-illuminated area as seen by the camera D_e. For a circularly-illuminated surface [8], one has:

$$\begin{aligned} dx &= \frac{1.22\lambda D}{D_e cos\vartheta} \\ dy &= \frac{1.22\lambda D}{D_e} \end{aligned} \tag{2}$$

with ϑ the angle between the camera and the optical axis (see Fig. 1).

In addition to the grain size, polarization characteristics can be extracted from the speckle image. Each illuminated sample responds differently to polarization of the incident light depending on its own distribution of particle sizes. This distribution determines the polarization of the diffused photons and the medium diffusion regime [9]. Polarization properties of the backscattered light, quantified by the degree of polarization, can trace back that distribution. This parameter is determined from the speckle mean intensity measurements using Eq.3:

$$DOP = \frac{I_{//} - I_{\perp}}{I_{//} + I_{\perp}} \tag{3}$$

where $I_{//}$ is the mean intensity measured at the camera surface when the polarization of the incident light is fully transmitted, and $I_{\perp}$ is the mean intensity when the transmitted light results from either a cross linear (in case of an incident linear polarization), or helicity-flipped circular polarization (in case of an incident circular polarization). DOP_L and DOP_C, respectively linear and circular polarization degrees, are thus determined. The determination of these two degrees allows one to assess the predominant type of particles or diffusers and to identify relative variations in their size in the medium [10]. One can distinguish three different medium configurations whose speckle signatures are presented in Table 1. For medium constituted by large particles - compared to the wavelength, the diffusion is predominately forwarded. Moreover, circular polarization states are less depolarized than linear polarization states after many

#171813 - $15.00 USD Received 13 Jul 2012; revised 30 Aug 2012; accepted 31 Aug 2012; published 3 Oct 2012

scattering events. A Mie scattering regime is then characterized by a positive circular polarization degree DOP_C which is greater than DOP_L. While, in case of small particles, the light is scattered with the same probability in any direction: the Rayleigh scattering regime is predominant. Linear polarization is less affected by the number of diffusions and appears to maintain its initial polarization more than the circular one affected by backscattering via helicity flipping. A negative degree of circular polarization, $DOP_C < 0$, is observed. In medium with a mixture of particle sizes, the polarimetric behavior is dominated by small diffusers: DOP_C decreases with the increase of their proportion. In this case, most of photons are diffused and depolarized at different rates.

Table 1. Characteristics of different diffusion media according to the scatterers size. $dx^{//}$ represents the speckle grain size when the axis of the polarizer and analyzer are parallel, and $dx^{\perp}$ corresponds to crossed axis.

Medium	dx_c	dx_L	Comparison between DOP_C and DOP_L	Diffusion regime
Small scatterers	$dx_C^{\perp} > dx_C^{//}$	$dx_L^{\perp} < dx_L^{//}$	$DOP_C < 0$ and $DOP_C < DOP_L$	Rayleigh
Large scatterers	$dx_C^{\perp} < dx_C^{//}$	$dx_L^{\perp} < dx_L^{//}$	$DOP_C > 0$ and $DOP_C > DOP_L$	Mie
Mixture	$dx_C^{\perp} > dx_C^{//}$	$dx_L^{\perp} < dx_L^{//}$	$DOP_C < 0$ and $DOP_C < DOP_L$	Rayleigh

3. Experimental method

Speckle, fluorescence and biochemical measurements are performed on a set of green Conference pears brought from a local supplier with a state of maturation slightly ahead (unripe). The pears are first sorted so that they are as homogeneous as possible and almost identical in terms of mass and maturity. They are left to ripen for 10 days at room temperature and their state of maturity is monitored during this period except the fifth day.

(i) Speckle setup:

Figure 1 presents the experimental speckle setup used in our experiments. A 7 mw He-Ne laser delivers a 1 mm wide linear polarized beam at I_0 / e^2 where I_0 is the maximum laser intensity at the 632.8 nm wavelength with a coherence length of about 20 cm. No beam expander is used in the setup. In that way, we can ensure that the backscattered laser spot on fruit depends only on diffusion properties inside the fruit, *i.e.* the maturity level. D_e variation and consequently the speckle grain size variation can thus be observed (Eq. 3). A CMOS camera is used to detect light diffused in the ϑ=45° direction with a 10 ms exposure time and a pixel size of 8μmx8μm. The distance D between the camera and the fruit is fixed at 27 cm. Polarizers and quarter-wave plates are used to ensure once a linear polarization of the incident laser beam and once a circular one. Three selected pears are studied by speckle measurements once per day. Each fruit is permanently mounted on a plate to illuminate the same area of the fruit, day after day, and thus ensure measurements repeatability. For each fruit, the speckle image is acquired, on two opposite faces, four times under different incident polarizations and polarization analysis conditions:
a) with a linearly polarized incident beam, the quarter wave plates are removed. A 0° or 90° rotation of the analyzer polarization axis, with respect to the entrance polarizer, is done to record the parallel image and the perpendicular image respectively [11]. $dx_L^{//}$ and $dy_L^{//}$ are the corresponding grain sizes measured in the case of parallel linear polarizers. $dx_L^{\perp}$ and $dy_L^{\perp}$ are calculated for the crossed polarizers axis case. DOP_L is estimated using Eq.3.

#171813 - $15.00 USD Received 13 Jul 2012; revised 30 Aug 2012; accepted 31 Aug 2012; published 3 Oct 2012

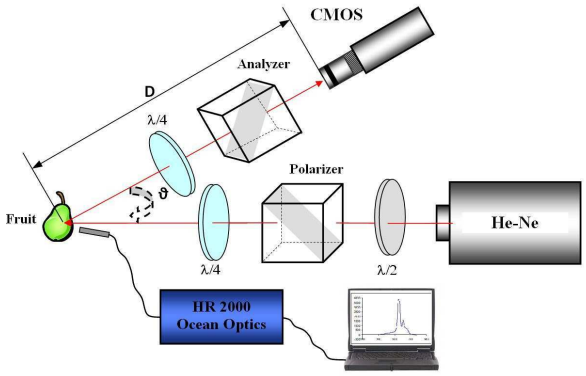

Fig. 1. Top view of the experimental setup. $\lambda/2$ and $\lambda/4$ are half and quarter wave plates.

b) with a circularly-polarized beam, the quarter-wave plates are kept. $dx_C^{//}$, $dy_C^{//}$, $dy_C^{\perp}$ and $dx_C^{\perp}$ are determined. DOP_C is also calculated using Eq.3.
For each of the three selected fruits, DOP and dx values corresponding to the two faces are averaged along the study.

(ii) Fluorescence setup:

Chlorophyll pigments, both chlorophyllα (Chlα) and chlorophyllβ (Chlβ), are the origin of plants greenness. Their breakdown mechanism exists not only in plants growth but also during fruits ripening. In other terms, the fruit is more or less rich in chlorophyll depending on its ripeness stage. The fluorescence study is based on the fluorescence of chlorophyll at 632 nm. These green pigments absorb radiation at 632 nm and fluoresce by emitting photons of wavelength 685 nm corresponding to chlorophyllα, and 735 nm corresponding to chlorophyllβ. The fluorescence peaks intensity named F685 and F735 are linearly related to the amount of green pigments [12]. The higher the Chlα content, the higher the F685. The same applies for Chlβ and the F735. Daily, a Ocean Optics spectrometer HR2000 registers the fluorescence intensity of chlorophyll of each of two faces of the three selected fruits (see the lower part of Fig.1). These two values are also averaged.

(iii) Biochemical measurements:

In addition to speckle and fluorescence measurements, two fruits are sacrificed daily for biochemical measurements of the inner content of fruits, including pigmentation and total soluble sugars (TSS) analysis. Hydrolysis of starch during ripening leads to break them down into constituent sugars whose concentrations increase during ripening. The dosage of TSS is done using Yemm and Willis [13] protocol: a 200 μL aliquot of the supernatant is mixed with 1 mL of anthrone-sulfuric reagent (0.1% anthrone and 0.1% thiourea in 12.5 N sulfuric acid) and incubated for 10 min at 100°C. After cooling, the absorbance is read at 625 nm and results are expressed in mg of glucose equivalent per g of dry weight (DW).
As for the pigmentation extraction procedure, it is carried out under low light intensity in order to minimize chlorophyll alteration [14]. Fruits peels are macerated for 30 mn at 4°C in 80% (v/v) acetone under gentle shaking, in the presence of 50 mg $MgCO_3$ to prevent chlorophyll acidification. The liquid phase is collected and kept at 4°C. Chls α,β and carotenoid concentrations are estimated spectrophotometrically according to the absorbance coefficients OD (optical density) determined by Lichtenthaler [15]. Results are expressed in mg per g of fresh weight

#171813 - $15.00 USD Received 13 Jul 2012; revised 30 Aug 2012; accepted 31 Aug 2012; published 3 Oct 2012

(FW). Weight ratio of Chls α and β to total carotenoid concentrations, an indicator of the greenness of plants, is also calculated. It is represented by $R_{Pigmentation}$: $R_{Pigmentation}=\frac{Chls\alpha+Chls\beta}{carotenoids}$. High values of this parameter indicate fruit greenness and its ripening level, while low values are a sign of fruits senescence.

4. Results

(i) Experimental results and interpretation:

We observe for each pear a continuous decrease of speckle grain size during the study. Results averaged on the three pears are illustrated in Fig. 2. During fruits ripening, speckle grain size decreases in linear or circular polarization and in both parallel and crossed acquisition, around 4 pixels between the first and the tenth day. A crossing between the circular parallel and the circular crossed grain sizes might have occurred after the third day and $dx_C^{\perp}$ becomes greater than $dx_C^{//}$ starting from that particular day. As the speckle size is an indicator for the medium scattering characteristics [10], this behavior in grain size ($dx_C^{\perp} > dx_C^{//}$) is the signature of a small scatterers presence and thus a predominant Rayleigh diffusion regime.

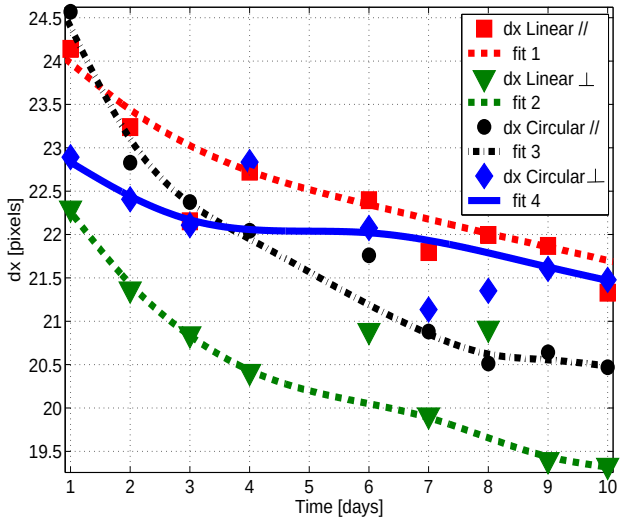

Fig. 2. Variation of horizontal speckle grain size during ripening. Results are averaged on the three monitored pears. Different symbols correspond to the four light polarization configurations. Dots represent experimental results; dashed lines represent the spline fit. dx error bars are on the order of 2 pixels and are not illustrated in the figure for clarity purpose.

According to Rayleigh-Gans theory [16], appropriate when $|\frac{n_p}{n_m}\text{-}1|<<1$, the reduced scattering coefficient μ_s' depends on the medium refractive index n_m and the particle refractive index n_p as follows:

$$\mu_s' = K(\frac{n_p}{n_m} - 1)^2 \tag{4}$$

K is the proportionality factor which takes into account particle size and density in the medium, wavelength of incident light and anisotropy factor g. In our experiments, TSS content in fruits increased during ripening as shown in Table 2, yielding to increase the medium refractive index [17]. Therefore μ_s' decreases leading to favored forward diffusion. The contributing volume increases in this case and the speckle grain size gets smaller [18].

#171813 - $15.00 USD Received 13 Jul 2012; revised 30 Aug 2012; accepted 31 Aug 2012; published 3 Oct 2012

Table 2. Evolution of Total Soluble Sugars level TSS during days.

Day	TSS (%DW)
1	17.37 ± 1.70
2	19.97 ± 2.58
3	20.48 ± 0.52
4	20.51 ± 3.75
6	21.67 ± 1.83
7	22.55 ± 1.76
8	21.80 ± 0.24
9	20.69 ± 1.76

As K also depends on particle size, the diffusers size variation during starch hydrolysis should also have an effect on μ_s'. Glucose concentration tends to decrease speckle grain size while the scatterers size decrease can enhance the retrodiffusion effect and so the speckle grain size. These effects can not be distinguished one from the other at this stage of our study. Additional experiments and simulations should be conducted to separate these two phenomena contributions with regard to the speckle grain size evolution.

Regarding the chlorophyll results, fluorescence and pigmentation analysis show a continuous degradation during ripening. Figure 3.a presents averaged fluorescence decay of F685 and F735

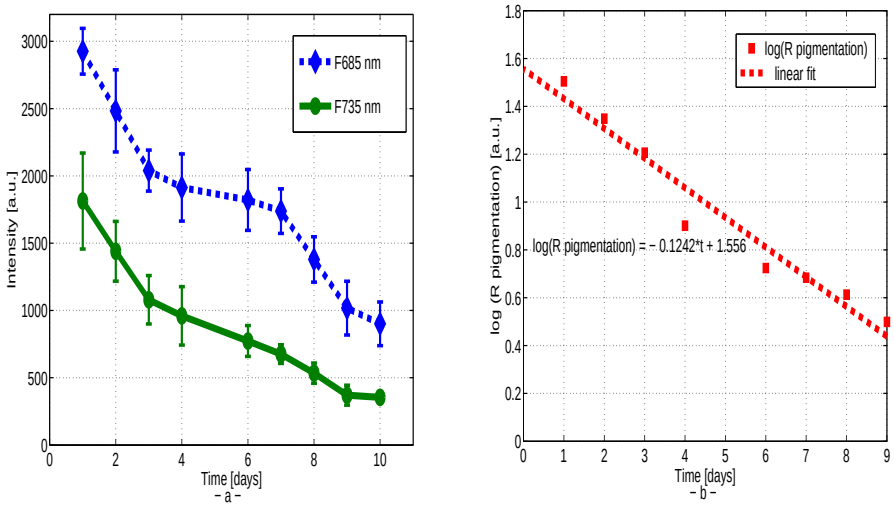

Fig. 3. -a- On the left, variation of the intensity peak at 685nm and 735nm during ripening. Results are averaged on the three monitored pears. Diamonds and dots represent the F685 and F735 intensities respectively. -b- On the right, variation of $R_{pigmentation}$ during ripening. Results are monitored on two pears. Squares represent the experimental logarithmic values of $R_{pigmentation}$ and the dashed line is the linear fit. Error bars in both plots correspond to the standard deviation.

along maturation. After ten days, F685 peak falls down from 3000 to 1000 a.u. and F735 peak decreases from 1800 to 400 a.u. A similar evolution is obtained for $R_{pigmentation}$ which shows

#171813 - $15.00 USD Received 13 Jul 2012; revised 30 Aug 2012; accepted 31 Aug 2012; published 3 Oct 2012

an exponential diminution as presented in Fig. 3.b.
Light diffusion in fruit is altered by the variation of chlorophyll concentration. These pigments represent the main absorbents at 635 nm, therefore their regression affects the absorption coefficient which is reduced as well. This leads to increase the illuminated backscattered volume on the fruit. In other terms, the illuminated volume becomes greater and speckle grains size, which is inversely proportional to the diffusion diameter spot D_e, is therefore smaller.
Although the simultaneous effects of the scatterers size and glucose concentration variations on the reduced scattering coefficient is not evident, one can reasonably assume that both diminution of absorption and reduced scattering coefficients can explain the observed fall down of the speckle grain size.

In order to investigate deeply scattering characteristics in the fruit during ripening and to assess the predominant type of backscattered photons, degree of polarization is evaluated. The circular and the linear polarization degrees continuously decrease along maturation as illustrated in Fig.4. During ripening, DOP_C remains always lower than DOP_L. After the third day DOP_C becomes negative, and follows an horizontal asymptote at -0.1.

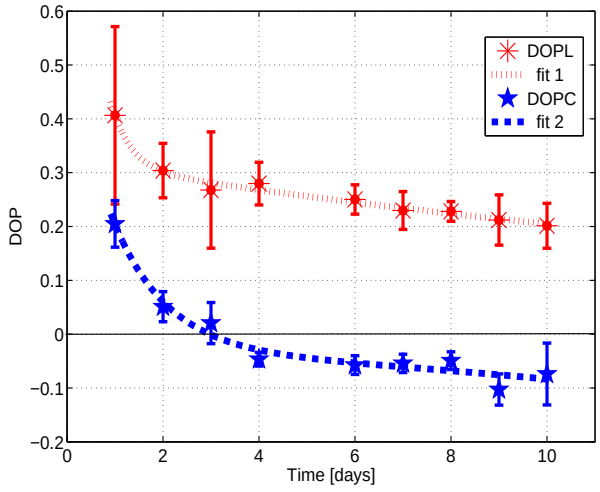

Fig. 4. Variation of DOP_C and DOP_L during maturation. Results are averaged on the three monitored pears. Dots represent experimental values and error bars correspond to the standard deviation. Dashed lines are the exponential fit.

For earlier days of ripening, between the first and the third day, most of the linearly polarized light maintains its original polarization state, giving us a high value of DOP_L. With ripening, fraction of light preserving its polarization state decreases, yielding to decrease DOP_L. The decrease of DOP_L becomes less important during the last stage of maturation. Whereas, for the circularly polarized light, at earlier days of ripening, the amount of photons maintaining polarization dominates those detected with helicity flipped, so DOP_C is positive. After the third day, DOP_C becomes negative: the helicity is flipped and the amount of depolarized circular light decreases (Fig. 4). This invokes a mirror effect as, starting from that day, the small diffusers contribution outweighs the large ones contribution.
The helicity flipping at the third day matches well with the cross between parallel and crossed circular grain size presented in Fig.2. The ratio DOP_C/DOP_L (R_{DOP}) decreases as well with

#171813 - $15.00 USD Received 13 Jul 2012; revised 30 Aug 2012; accepted 31 Aug 2012; published 3 Oct 2012

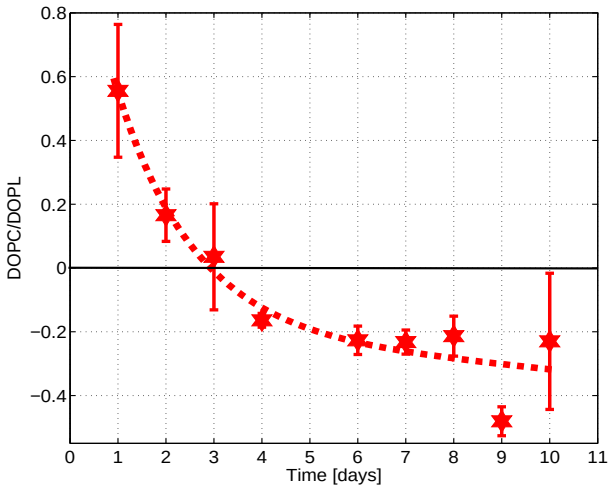

Fig. 5. Variation of the DOP_C/DOP_L ratio during maturation. Results are averaged on the three monitored pears; error bars correspond to the standard deviation.

time and its sign flips around the third day as shown in Fig. 5.
Simultaneously to glucose level evolution during ripening (Table 2), the decrease in both grain size and polarization degrees reflect the fruit diffusion regime. This medium presents an important growth of small scatterers concentrations between the first and the fourth day. All these observations seem to indicate that the fruit is characterized by a Rayleigh diffusion regime dominated by small scatterers.

(ii) Principal Component Analysis:

In order to highlight correlation between experimental parameters (DOP_C, DOP_L, F685, F735, dx, $R_{pigmentation}$ and TSS) and further validate speckle technique as a new method to monitor fruit maturation, a statistical study based on these variables is performed [19]. Principal Component Analysis (PCA) method is a multivariate statistical method, based on calculation of means, variances and correlation coefficients. This approach emphasizes similarities or contrasts between variables, marks the most correlated ones and measures the linear relationship between them. It is a method of identifying patterns in data and expressing it in a way to show similarities and dissimilarities by extracting the important information, correlating variables from the data table and expressing this information as a set of new orthogonal uncorrelated variables called principal components PC1, PC2, PC3 etc. In our case, the calculus is performed using the XLSTAT program. In the observation table, we report as variables all parameters extracted from speckle image, fluorescence and biochemical parameters along maturation period. Ripening days are the observations in this PCA approach.
Table. 3 presents the correlation coefficients between the different variables. A positive high correlation exists between DOP_L or DOP_C on one hand and fluorescence peak intensities (F685, F785) or $R_{pigmentation}$ on the second one. Similar correlation is established for the horizontal linear grain size in crossed/parallel configurations. As for the TSS, it is highly negatively correlated to speckle variables. Loadings of each of these variables projected on PC1 and PC2 axis are presented in Fig. 6. The Pearson circle of correlation presents variables according to their correlation to the major components: V= X*PC1+Y*PC2 with X, Y their representation

#171813 - $15.00 USD Received 13 Jul 2012; revised 30 Aug 2012; accepted 31 Aug 2012; published 3 Oct 2012

Table 3. Pearson correlation coefficient matrix between speckle variables, fluorescence and biochemical variables.

	DOP_L	DOP_C	DOP_C/DOP_L	$dx_L^{//}$	$dx_L^{\perp}$	F685	F735	TSS	$R_{pigmentation}$
DOP_L	1	-	-	-	-	-	-	-	-
DOP_C	0.961	1	-	-	-	-	-	-	-
DOP_C/DOP_L	0.936	0.979	1	-	-	-	-	-	-
$dx_L^{//}$	0.968	0.895	0.871	1	-	-	-	-	-
$dx_L^{\perp}$	0.862	0.888	0.911	0.847	1	-	-	-	-
F685	0.927	0.916	0.955	0.892	0.863	1	-	-	-
F735	0.956	0.945	0.971	0.929	0.863	0.984	1	-	-
TSS	-0.907	-0.867	-0.804	-0.891	-0.698	-0.733	-0.831	1	-
$R_{pigmentation}$	0.914	0.944	0.971	0.871	0.832	0.940	0.978	-0.845	1

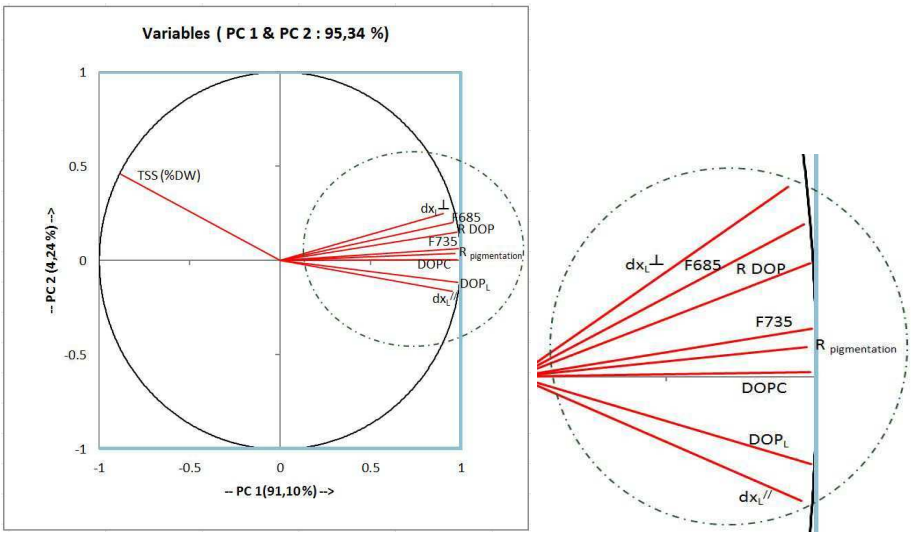

Fig. 6. Pearson circle correlation presenting loadings of variables projected on PC1 and PC2 axis. The right part of the figure presents a zoom of the encircled zone.

percentage on each component. Variables are 91.10% expressed by the first component PC1 and 4.24% by the second one. $R_{pigmentation}$, F685 and F735 lie, along PC1, close to $dx_L^{//}$, $dx_L^{\perp}$, DOP_L and DOP_C and their corresponding ratio and close to the horizontal axis, meaning that they are highly positively correlated. TSS(%DW) lies in the fourth quadrant. In another words, it is highly negatively correlated to the speckle parameters. These two ways of presenting variables show the absolute positive high correlation between speckle grain size and polarization degrees with chlorophyll content on one hand and total soluble sugars content on the other one. Furthermore, this statistical method allows to present observations *i.e.* the days of maturation in a new plot according to their correlation to the principal components as represented in Fig. 7. These days are separated into two groups: first, second and third days in the right side, and the rest in the left side. The switch between the third and the fourth day reminds the speckle grain sizes cross (Fig. 2) and the DOP_C sign flip (Fig. 4). It is also relevant to stress on their ascending

#171813 - $15.00 USD Received 13 Jul 2012; revised 30 Aug 2012; accepted 31 Aug 2012; published 3 Oct 2012

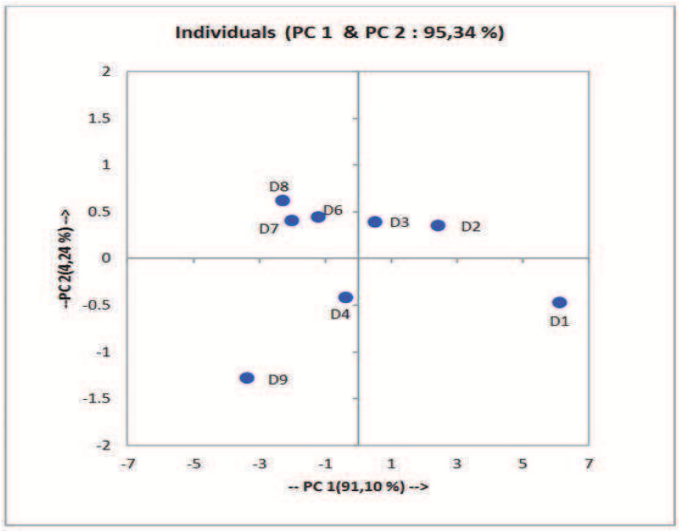

Fig. 7. Observations grouped according to the maturation level starting from day one till day nine.

order from the right to the left side of the plot. Using PCA technique, our observations are well distinguished one from the other. The ripeness level of Conference pears is evaluated at 91% using speckle variables.

5. Conclusion

We performed backscattered speckle images on fruits during ripening process along with fluorescence and biochemical measurements. We showed that as the glucose content is increasing, DOP_C reaches negative values and $\mathrm{dx}_C^{\perp}$ becomes greater than $\mathrm{dx}_C^{//}$. This signature is proper to medium constituted of a significant part of small scatterers where Rayleigh diffusion regime overweighs Mie regime. In addition, the continuous decrease of dx along maturation can be attributed either to μ_s' via the scatterers size and glucose concentration or μ_a via the pigmentation level. However, our experiments can not discriminate the absorption contribution from the diffusion one on the speckle grain size.

Simultaneously, we carried out principal component analysis on all parameters extracted from the speckle image, the fluorescence and the biochemical measurements. This statistical analysis showed a high correlation between variation in the speckle image on one side, and the inner variation in the fruit on the other side.

We are currently carrying out speckle theoretical studies based on Monte Carlo simulations taking into account light polarization and media characteristics. Such simulations could be used to discriminate and quantify diffusion coefficient variations effect from the absorption one on the fruits speckle image.

Acknowledgment

The authors thank the “Agence Universitaire de la Francophonie-Bureau du Moyen Orient” for funding the project.

#171813 - $15.00 USD Received 13 Jul 2012; revised 30 Aug 2012; accepted 31 Aug 2012; published 3 Oct 2012